applied sciences

MDPI

Article

Uncovering the Use of Fucoxanthin and Phycobiliproteins into Solid Matrices to Increase Their Emission Quantum Yield and Photostability

Lília M. S. Dias [1], Gabriela Kovaleski [1,2], Lianshe Fu [1,*], Tânia R. Dias [3], Inês P. E. Macário [2,3], Sandra F. H. Correia [4], Joana L. Pereira [3], João A. P. Coutinho [2], Sónia P. M. Ventura [2] and Rute A. S. Ferreira [1,*]

[1] Department of Physics and CICECO—Aveiro Institute of Materials, University of Aveiro, 3810-193 Aveiro, Portugal; liliadias@ua.pt (L.M.S.D.); gabrielak@ua.pt (G.K.)
[2] Department of Chemistry and CICECO—Aveiro Institute of Materials, University of Aveiro, 3810-193 Aveiro, Portugal; inesefe@ua.pt (I.P.E.M.); jcoutinho@ua.pt (J.A.P.C.); spventura@ua.pt (S.P.M.V.)
[3] Department of Biology and CESAM—Centre for Environmental and Marine Studies, University of Aveiro, 3810-193 Aveiro, Portugal; dias.t@ua.pt (T.R.D.); jpereira@ua.pt (J.L.P.)
[4] Instituto de Telecomunicações and University of Aveiro, Campus Universitário de Santiago, 3810-193 Aveiro, Portugal; sandracorreia@ua.pt
* Correspondence: lianshefu@ua.pt (L.F.); rferreira@ua.pt (R.A.S.F.)

Abstract: In the search for a better and brighter future, the use of natural luminescent renewable materials as substitutes for synthetic ones in the energy field is of prime importance. The incorporation of natural pigments (e.g., xanthophylls and phycobiliproteins) is a fundamental step in a broad spectrum of applications that are presently marred by their limited stability. The incorporation of bio-based luminescent molecules into solid matrices allows the fabrication of thin films, which may dramatically increase the range of applications, including sustainable photovoltaic systems, such as luminescent solar concentrators or downshifting layers. In this work, we incorporated R-phycoerythrin (R-PE), C-phycocyanin (C-PC), and fucoxanthin (FX) into poly(vinyl alcohol) (PVA) and studied their optical properties. It was found that the emission and excitation spectra of the phycobiliproteins and FX were not modified by incorporation into the PVA matrix. Moreover, in the case of FX, the emission quantum yield (η) values also remained unaltered after incorporation, showing the suitability of the PVA as a host matrix. A preliminary photostability study was performed by exposing the solid samples to continuous AM1.5G solar radiation, which evidenced the potential of these materials for future photovoltaics.

Keywords: luminescence; luminescent solar concentrators; luminescent downshifting layers natural pigments; polymer; xanthophyll; phycobiliprotein

Citation: Dias, L.M.S.; Kovaleski, G.; Fu, L.; Dias, T.R.; Macário, I.P.E.; Correia, S.F.H.; Pereira, J.L.; Coutinho, J.A.P.; Ventura, S.P.M.; Ferreira, R.A.S. Uncovering the Use of Fucoxanthin and Phycobiliproteins into Solid Matrices to Increase Their Emission Quantum Yield and Photostability. *Appl. Sci.* **2022**, *12*, 5839. https://doi.org/10.3390/app12125839

Academic Editor: Marilena Carbone

Received: 3 May 2022
Accepted: 5 June 2022
Published: 8 June 2022

1. Introduction

In the energy field, most of the luminescent materials used are based on quantum dots (QDs), lanthanides, and synthetic dyes [1], which often involve complicated/harsh synthesis conditions or are non-recyclable [2,3]. Although the amount of luminescent material for such applications is typically low (<0.5% wt), they may have toxic effects on certain organisms, namely those in the aquatic compartment by causing significant alterations in the ecological conditions of the aquatic fauna and flora because of their non-biodegradable nature, which means a negative impact on the equilibrium of the aquatic environment. Moving towards a more sustainable future requires the use of natural materials to replace synthetic ones, enabling the fabrication of sustainable and cheap photovoltaic (PV) systems, such as luminescent solar concentrators (LSCs) or downshifting layers, as well as keeping other inherent features such as synthetic versatility, high absorption coefficients, and quantum yield values [4]. Solar harvesting and converting materials are one relevant

class of biomolecules [5] able to open new perspectives in the field of building-integrated PVs [1,6], through LSCs [1,7–11]. Benefiting from their high absorption coefficient and emission quantum yields, the LSCs are planar waveguides that collect sunlight at the surface and concentrate it into the low area of the edges, where PV cells are applied. The light conversion is mediated by a down-shifting mechanism of the solar radiation, whose performance under diffuse light conditions is an advantage [1,12]. Examples of bio-based LSCs include the use of phycobiliproteins [13–15], chlorophyll [16], green fluorescent protein (GFP) [5,17], and C-phycocyanin (C-PC) [5] with competitive performance compared to those based on synthetic dyes [6]. In these cases, the bio-molecules are used mainly in solution to preserve their intrinsic chemical stability. To enlarge the application range and the processing, the incorporation into solid matrices is a relevant step that has been challenging, as optical performance decreases induced by aggregation [18]. In parallel with performance, challenges for bio-luminescent materials also include the emission red-shift towards the red/NIR spectral region, in resonance with the Si-based PV cells absorption.

To incorporate luminescent natural molecules into solid matrices and retain the optical properties/long-term viability, the following issues should be considered: (i) the microenvironment of solid hosts should be similar to or mimic the native environment of the molecules, while simultaneously providing a rigid structure, (ii) the entrapment process should be performed at room temperature, (iii) the bio-molecules usually require neutral solutions, acidic and basic environments should be avoided, and (iv) effects of solvents and ionic strength of the solution should be considered [19]. In this context, several attempts have been done, namely by investigating the use of encapsulation strategies such as sol-gel derived SiO_2 material from tetramethoxysilane [20], and hybrid matrices [21] using polymer additives dispersed into sol-gel processed materials derived from tetraethyl orthosilicate alone or copolymerized with methyltriethoxysilane or dimethyldimethoxysilane [21]. Chen and co-authors encapsulated different phycobiliproteins (R-phycoerythrin; R-PE, C-PC, and allophycocyanin; APC) in sol-gel glasses and discovered that the impact on the spectroscopic properties was significantly distinct. While C-PC and APC changed in terms of agglomeration and conformation, R-PE only suffered minor changes and revealed fluorescence [22]. More recently, Bharmoria et al., proposed a sustainable strategy for overcoming the R-PE photochemical stability limitations by embedding it in gelatin in a solid-state [18]. Other works reporting the encapsulation strategy used natural or synthesized hydrophilic polymers, namely calcium alginate (protects the nativity of the protein and its structure at high temperature) [23], polyacrylamide films entrapped with phycobilisomes for LSCs [13] or metal-organic frameworks (MOFs) [24]. As an example, R-PE was incorporated into a blue MOF thin film through a solid-confinement conversion process [24]. Nevertheless, R-PE was denatured and exhibited dual-color fluorescence emission including green and red light, while the original single orange light was significantly suppressed [24]. Finally, also FX stability was assessed under encapsulation in polyvinylpyrrolidone nanoparticles [25] or PVA and poly(D,L-lactic-co-glycolic acid) microspheres [26]. In line with the recent interest in biomolecules for solar-based applications, namely solar harvesting sensors [5] and LSCs [6], the interest in new biomolecules with enhanced solar absorption and conversion and stability gained visibility.

This study aimed to improve the optical properties and long-term viability of phycobiliproteins (R-PE, C-PC) and FX from marine sources through entrapment into solid matrices (PVA and sodium alginate). The rationale for the selection of these nature-based optically active centers lies in the fact that they present emission in the red spectral region, matching c-Si PV devices' maximum absorption. Their incorporation yields luminescent materials with emission features analogous to those of the biomolecules in the solution. Moreover, the materials revealed promising photostability results under solar irradiation prospecting its use in energy-harvesting applications, such as down-shifting layers and LSCs.

2. Materials and Methods

2.1. Materials

Ethanol (analytical reagent grade, Fisher Scientific, Portugal), ammonium sulfate (99%, Panreac), poly(vinyl alcohol) (n = 1750 ± 50, PVA, TCI Europe N.V., Zwijndrecht, Belgium), and sodium alginate (Aldrich, Steinheim, Germany) were used as purchased.

2.2. Methods

2.2.1. Preparation of R-PE Extracts

R-PE was extracted from the red macroalgae *Gracilaria gracilis*, which were kindly provided by ALGAplus (Ílhavo, Portugal). The fresh algae were left to dry at room temperature over absorbent paper. Then, 20 g of algae were weighed, placed into a mortar for maceration with liquid nitrogen, and further ground to a powder using a coffee mill. Afterward, the algae powder was dissolved in 40 mL of distilled water and homogenized in an orbital shaker for 20 min, at 250 rpm and room temperature. The extract was then filtered to remove large debris and centrifuged at 12,000 rpm for 10 min, at room temperature. In the end, the supernatant was isolated and the pellet discarded.

2.2.2. Preparation of C-PC Extracts

C-PC was extracted from an in-house culture of the cyanobacterium *Anabaena cylindrica*. Cultures were incubated in glass flasks with Woods Hole MBL medium [27] and kept at 20 ± 2 °C, with photoperiodic lighting (16 h of light:8 h of dark) provided by cool white fluorescent tubes (2300 lx). The biomass was harvested from 13-day-old cultures, recovered through centrifugation at 4000 rpm, and stored at −20 °C until further use. For C-PC extraction, the frozen biomass was weighted, left at room temperature for 90 min protected from light, and then dissolved in sodium phosphate buffer (150 mM, pH 7) in a solid–liquid ratio of 100 mg of biomass *per* mL of buffer. The homogenate was incubated at 35 °C for 50 min, in a microtube Thermomixer (Eppendorf 5535R), with a mixing frequency of 1500 rpm. The homogenate was centrifuged at 12,000 rpm, for 10 min, at room temperature, using a VWR microstar 17 centrifuge. The supernatant was isolated to obtain the C-PC extract, while the pellet was discarded.

2.2.3. Preparation of FX Ethanolic Extracts

FX was extracted from the microalga *Isochrysis galbana* Parke 1949, and purchased from Necton S.A. (Olhão, Portugal) [28]. The batch was produced in photobioreactors systems (PhytoBloom), then freeze-dried, ground into powder, and kept in a dry and dark environment until use. Pure ethanol was the solvent used for the solid–liquid extraction (solid–liquid ratio of 0.01 g of algae powder *per* mL of pure ethanol) of FX. The sample homogenization was carried out protected from light in a digital overhead shaker (IKA TRAYSTER, Staufen, Germany) with a constant vertical rotation of 80 rpm for 30 min, at room temperature. Afterward, the extract was centrifuged (Thermo Scientific Heraeus Megafuge 16R, Waltham, MA, USA) at 5000 rpm, for 30 min at 4 °C, the supernatant was recovered to a new tube, while the biomass pellet was discarded. Since the supernatant contained not only the carotenoid of interest FX but also chlorophylls, thus a pre-washed and dried resin (AmberLite™ HPR900 OH from Fisher Scientific, CAS 9017-79-2, Hampton, VA, USA) was used to isolate FX [28]. The resin was mixed with the extract (0.15 g of resin *per* mL of extract) for 30 min, at room temperature, in a magnetic stirrer, so that the resin could adsorb the chlorophyll content. The organic liquid fraction containing the carotenoid was collected with a syringe and the resin was discarded. Although *Isochrysis galbana* contains different xanthophylls, the total recovered xanthophylls by this method were regarded as FX. Absorbance at 450 nm was read using a UV-Vis microplate reader (Synergy HT microplate reader, BioTek, Winowski, VT, USA). The samples were analyzed in duplicate, and pure ethanol was used as a blank. The concentration ($\mu g \cdot mL^{-1}$) was calculated using previously defined calibration curves (y = 0.0432x, R^2 = 0.999, Figure S1a in Supplementary Materials).

2.2.4. Purification of R-PE and C-PC Aqueous Extracts

For the extracts' purification, 20% (w/v) of ammonium sulfate was added to each sample, homogenized, and kept overnight at 4 °C to allow the protein precipitation. On the following day, samples were centrifuged at 3000 rpm for 15 min, at room temperature. The supernatant was discarded, and the pellet was re-suspended in ultrapure water. Absorbance at 565 or 615 nm was read for R-PE or C-PC analysis, respectively, using a UV-Vis microplate reader (Synergy HT microplate reader, BioTek). Samples were analyzed in duplicate, and ultrapure water was used as a blank. The concentration ($mg \cdot mL^{-1}$) was calculated using previously defined calibration curves (y = 5.1108x, R^2 = 0.999 for R-PE and y = 0.479x, R^2 = 0.991 for C-PC, Figure S1b,c in Supplementary Materials).

2.2.5. Incorporation of R-PE, C-PC, and FX in Host Solid Matrices

Aqueous solutions of R-PE (0.215 $mg \cdot mL^{-1}$) and C-PC (2.6 $mg \cdot mL^{-1}$) and ethanolic solution of FX (0.031 $mg \cdot mL^{-1}$) were applied. Distilled water was used throughout the experiments. PVA (10%, w/w) was prepared by adding 50 mL of water to 5.0 g of PVA. The resulting solution was heated at 90 °C for 2 to 3 h, and then a clear viscous solution was obtained. The incorporation of R-PE in sodium alginate was performed by adding 0.5 g of sodium alginate to 9.5 mL of water. The mixture was stirred at room temperature to get a clear viscous solution. Then, 400 µg of R-PE aqueous solution was added and stirred. The solution was placed at 35 °C to obtain an R-PE/alginate film. For the R-PE/PVA film, 5.5 g of PVA solution (10%, w/w) was mixed with 0.40 mg of R-PE stock solution and stirred to get a homogeneous solution. The resulting solutions were dried at 35 °C in an oven. The C-PC/PVA sample was obtained by adding 1.2 mg of C-PC solution to 5.5 g of PVA aqueous solution (10%, w/w), and the mixture was stirred at room temperature and placed at 35 °C to obtain the C-PC/PVA film. The FX/PVA sample was obtained by adding 0.05 mg of FX ethanolic solution to 5.5 g of PVA aqueous solution (10%, w/w), with the mixture stirred at room temperature. The solution was placed at 35 °C for obtaining the FX/PVA film.

2.2.6. Optical Characterization

The emission and excitation spectra were recorded at room temperature using a Fluorolog3® Horiba Scientific (Model FL3-22) spectroscope, with a modular double grating excitation spectrometer (fitted with 1200 $grooves \cdot mm^{-1}$ grating blazed at 330 nm) and a TRIAX 320 single emission monochromator (fitted with 1200 $grooves \cdot mL^{-1}$ grating blazed at 500 nm, reciprocal linear density of 2.6 $nm \cdot mm^{-1}$). The excitation source was a 450 W Xe arc lamp. The emission spectra were corrected for detection and optical spectral response of the spectrofluorimeter and the excitation spectra were corrected for the spectral distribution of the lamp intensity using a photodiode reference detector. Emission decay curves were recorded at room temperature on a Fluorolog TCSPC spectrofluorometer (Horiba Scientific, Piscataway, NJ, USA) coupled to a TBX-04 photomultiplier tube module (950 V). The exciting source was a Horiba/Jobin–Yvon pulsed diode (NanoLED-390, peak at 388 nm). The absolute emission quantum yield values were measured at room temperature using a quantum yield measurement system C9920-02 from Hamamatsu. This system consists of a Xe arc lamp (150 W), a monochromator (bandwidth 2 nm), an integrating sphere made of Spectralon® (99% reflectance for wavelengths within 350–1650 nm) with an inner diameter of 84 mm, and a multichannel detector (wavelength resolution < 2 nm). The emission quantum yield (η) is given by:

$$\eta = \frac{N_{Emi}}{N_{Abs}} = \frac{\int_{\lambda_1}^{\lambda_2} \frac{\lambda}{hc}\left[I_{em}^{sample}(\lambda) - I_{em}^{reference}(\lambda)\right] d\lambda}{\int_{\lambda_3}^{\lambda_4} \frac{\lambda}{hc}\left[I_{ex}^{sample}(\lambda) - I_{ex}^{reference}(\lambda)\right] d\lambda} \quad (1)$$

where N_{Abs} and N_{Em} are the numbers of photons absorbed and emitted by a sample, respectively, h is Planck's constant, c is the velocity of light, I_{em}^{sample} and $I_{em}^{reference}$ are the

emission intensities the measured with and without a sample, respectively, in the emission spectra wavelength interval [λ_1,λ_2] and I_{ex}^{sample} and $I_{ex}^{reference}$ are the integrated intensities of the excitation radiation measured with and without a sample, respectively, in the excitation wavelength interval [λ_3,λ_4] [29]. Three measurements were made for each sample, and the average values obtained are reported with an accuracy of 10% according to the manufacturer.

3. Results and Discussion

The photoluminescence of the polymeric materials was found similar to that of the bio-molecules in solution [15] under UV irradiation (Figure 1). Figure 2a shows the emission spectra of the R-PE/PVA dominated by the R-PE characteristic emission (Figure S2 in Supplementary Materials) with two components centered around 577 nm and 663 nm [15,30], which are independent of the excitation wavelength (Figures S3 and S4 in Supplementary Materials). The presence of two distinct dye-related components in the emission spectra points out the formation of dye aggregates [15,31] and the increase in the relative intensity of the low-energy component (663 nm), suggests the presence of *J*-dimers [15,32]. Both in R-PE/PVA and R-PE/alginate, the high-wavelength peak is red-shifted from 650 nm before incorporation (Figure 3a) to 665 and 663 nm after incorporation into PVA and sodium alginate (Figures S3 and S4 in Supplementary Materials), respectively, suggesting the formation of protein agglomerates in the solid-state.

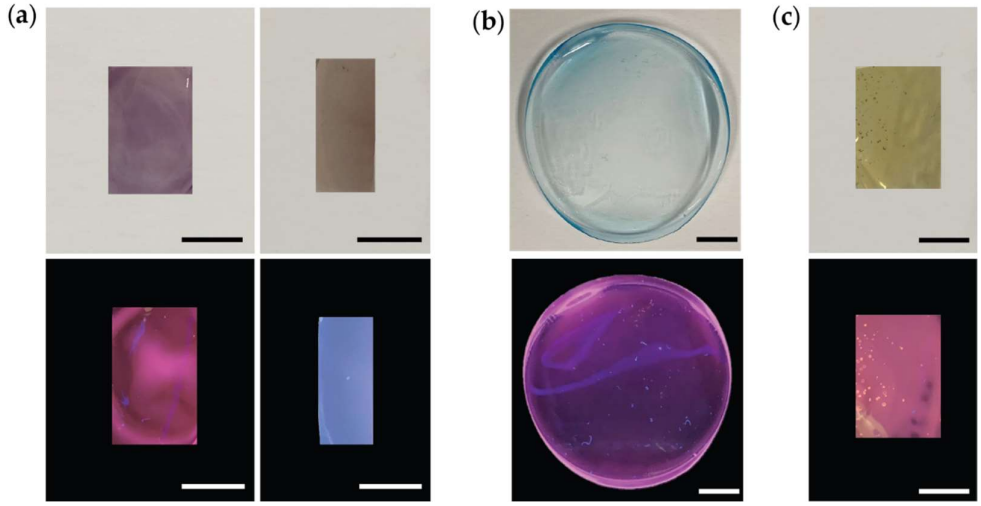

Figure 1. Photographs of (**a**), from left to right, R-PE/PVA and R-PE/alginate, (**b**) C-PC/PVA, and (**c**) FX/PVA under white light (**top**) and UV irradiation at 365 nm (**bottom**). Scale bars: 10^{-2} m.

The emission spectra of C-PC in H_2O (Figure 3a and Figure S5 in Supplementary Materials) for excitation wavelengths between 360 and 590 nm are formed by a component between 600 and 750 nm, with a peak at 674 nm, and a band with smaller relative intensity within 400 and 550 nm (Figure S5 in Supplementary Materials) [5,31]. After incorporation into PVA, the emission remains dominated by C-PC characteristic emission as given by the peak around 665 nm (Figure 2a) [31], revealing an increase in the relative intensity of the component at shorter wavelengths (Figure S6 in Supplementary Materials). The FX in solution and incorporated in thin films of PVA reveal emission when excited in the UV range (Figure 1c).

The emission spectrum of the FX in ethanol shows an emission band between 650 and 750 nm, with a peak at 675 nm, and a component with lower relative intensity between 500 and 650 nm (Figure 3a and Figure S7 in Supplementary Materials). The spectra are identical for excitation wavelengths between 350 and 600 nm (Figure S7 in Supplementary Materials). After incorporation into PVA, the emission spectra show a main band peaking around 675 nm (Figure 2a and Figure S8 in Supplementary Materials) and an increase in the relative

intensity of the band at shorter wavelengths (Figure S8 in Supplementary Materials). The excitation spectra revealed the same components both for FX in ethanol and incorporated into PVA, as presented in Figure 2b, Figures S7 and S8 in Supplementary Materials. These results show that the tested molecules preserve their emission and excitation features after incorporation into solid matrices and that the emission and excitation spectral regions are compatible with c-Si PV cells absorption and the available solar photons on earth, respectively (Figure 2). We notice that FX is mainly excited in the UV spectral region ensuring a larger Stokes shift suggesting that self-absorption could be minimized.

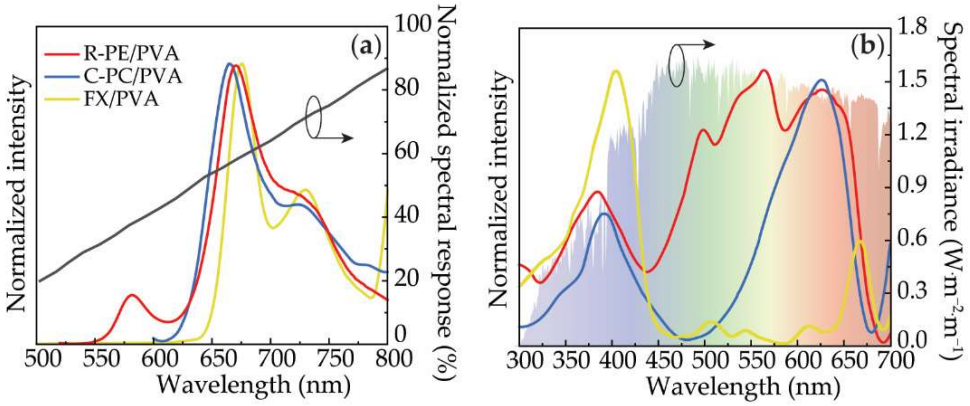

Figure 2. (**a**) Emission spectra for R-PE/PVA, C-PC/PVA, and FX/PVA excited at 498, 575, and 405 nm, respectively. The c-Si spectral response is shown on the right *y*-axis. (**b**) Excitation spectra for R-PE/PVA, C-PC/PVA, and FX/PVA monitored at 720 nm. The shadowed area represents the AM1.5G solar spectrum (right *y*-axis).

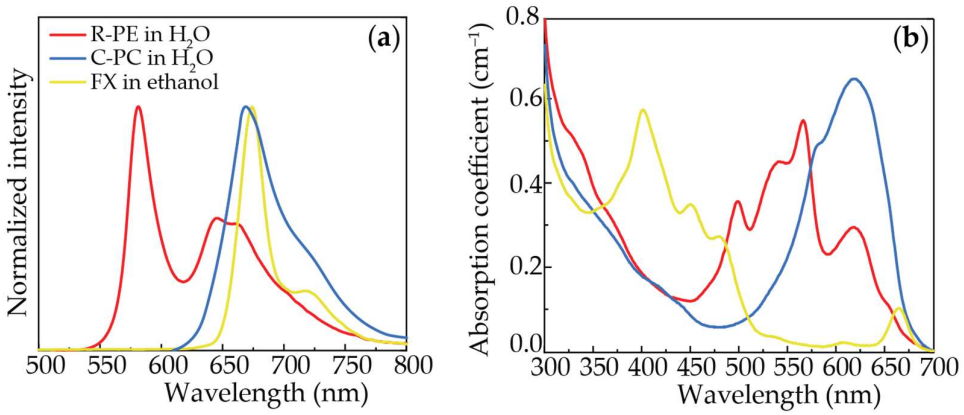

Figure 3. (**a**) Emission upon excitation at 488, 590, and 410 nm, respectively, and (**b**) absorption spectra of the bio-molecules R-PE, C-PC, and FX in solution.

The ability to down-shift the UV radiation arises from the intrinsic absorption of the bio-molecules in solution, as illustrated in Figure 3b. These absorption features are kept after incorporation into the host. In particular, the excitation spectra of R-PE after incorporation into PVA or sodium alginate also resemble that of the biomolecules (Figure 3b, Figures S3 and S4 in Supplementary Materials), being dominated by the excited states of the R-PE in the visible spectral range, revealing the presence of components in the UV/blue (320–440 nm) spectral region attributed to the chromophores' singlet states [15]. It should be noted that, under UV excitation, the emission spectra of R-PE/PVA and R-PE/alginate samples also reveal a component within the 400–550 nm range, which is more prominent than the R-PE characteristic emission in the case of the sodium alginate sample. Since for PV applications, the emission of the optically active materials should be mainly in the red/NIR spectral region (matching c-Si maximum absorption, Figure 2a), PVA was selected as the main host matrix in this work. The excitation spectra of C-PC-based samples are

formed by a main C-PC-related component around 620 nm, showing no relevant changes after incorporation into PVA (Figure 2b).

The fluorescence decay curves of all samples revealed a single-exponential decay (Figures S9–S11 in Supplementary Materials). The lifetime values of R-PE in H_2O and R-PE/PVA were similar to that previously reported for the aqueous solution of R-PE [18]. A significant increase in the emission lifetime was found for the R-PE/alginate sample, although lower than that found for R-PE dispersed in gelatin [18]. In this case, such an increase was explained by the dispersion of the molecules in the film, which reduced the number of molecule–molecule non-radiative interactions, concomitantly increasing the lifetime [18,33]. For the C-PC based samples, the lifetime values found for C-PC in H_2O were similar to the one recently reported for an aqueous solution of C-PC [5], which was further enhanced when incorporated in the PVA matrix. In the case of FX, the lifetime values showed a slight decrease when incorporated in the PVA, compared to that found for the FX in ethanolic solution (Table S1 in Supplementary Materials).

The emission features were further quantified by the measurement of the absolute emission quantum yield (η, Table 1 and Table S1 in Supplementary Materials) for excitation wavelength around the excitation maxima. For the samples in solution, the maximum η values obtained for R-PE and C-PC in H_2O were 0.20 ± 0.02 and 0.17 ± 0.02, respectively, which are consistent with previously reported values [5,15]. For the FX in ethanol, the value found was 0.08 ± 0.01. After incorporation, the η of the R-PE decreases both for PVA and alginate samples, being the maximum η value measured for the R-PE-based samples (Table 1). Additionally, for the C-PC/PVA, the η is lower when compared to the value found for the aqueous solution (Table 1), suggesting aggregation, as already reported for the incorporation of R-PE in gelatin films [18,34]. For the case of the FX samples, the η values remain constant (0.08 ± 0.01 in solution to 0.10 ± 0.01 after incorporation into PVA), likely because FX is a xanthophyll that does not suffer aggregation.

Table 1. Absolute emission quantum yield (η) for the indicated excitation wavelengths (λ_{exc}) and emission lifetime values (τ), calculated from the best fit of the decay curves shown in Figures S9–S11 in Supplementary Materials.

Sample	λ_{exc} (nm)	η	τ (ns)
R-PE/PVA	498	0.11 ± 0.01	3.74 ± 0.03
C-PC/PVA	580	0.09 ± 0.01	4.30 ± 0.04
FX/PVA	610	0.10 ± 0.01	6.68 ± 0.02

To infer the photochemical stability of the solid samples at room temperature, the η values were measured after 6 months of storage at ambient light-exposed conditions. It was found that the values remain similar to the ones measured for the as-prepared samples (Table S2 in Supplementary Materials), thus demonstrating their optical stability. Additionally, prospecting future PV applications, the η values measurements were performed after continuous exposure to AM1.5G irradiation (Figure 4 and Table S2 in Supplementary Materials). The results showed that the most stable sample is the FX/PVA, with a decrease of about 40% of the initial η values after 960 min of exposure. Concerning the samples incorporating the phycobiliproteins, it was found that, although the R-PE/PVA sample lost around 50% of its initial η value in the first 120 min (poor result compared to that found previously concerning R-PE dispersed in gelatin [18]), the η value remained constant after that, reinforcing the suitability of PVA as a host matrix. Although the previous results were somehow promising, the C-PC/PVA sample lost all its emission after the 960 min of AM1.5G exposure, suggesting aggregation or UV-induced molecular degradation.

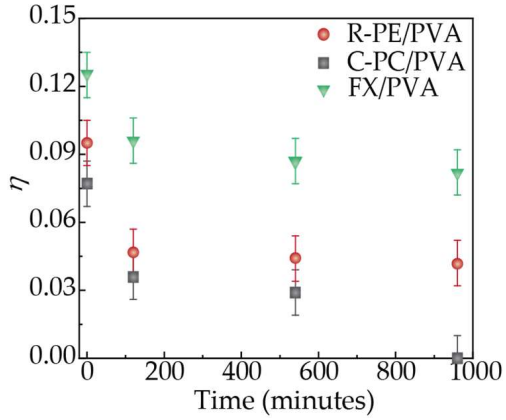

Figure 4. Time-dependent η values of the solid samples upon continuous exposure to an AM1.5G solar simulator for 960 min.

We note that very few works report the incorporation of nature-based molecules in solid matrices for application in LSCs. Nevertheless, works reporting the incorporation of phycobiliproteins in acrylamide [13] and gelatin hosts [18] resulted in materials with lower η values (~50% drop) than those of the phycobiliproteins dispersed in a liquid medium. Additionally, photostability studies under AM1.5G continuous exposure showed similar behavior to that in Figure 4 for phycobiliproteins [18]. Other molecules such as GFP [17] and chlorophyll [16] were incorporated into solid organic-inorganic matrices. For the case of chlorophyll, the η values were analogous to that measured for the diluted chlorophyll solution, pointing out that the incorporation did not contribute to an emission quenching and that the optical properties of the extract were well preserved in the solid state [16]. This was not the case with the GFP-doped organic–inorganic hybrid, which revealed a ~35% drop in the η values compared to that of the GFP aqueous solution [17]. The incorporation of chlorophyll in the solid matrices yielded photostable materials which showed a minor relative variation in the short-circuit current of coupled PV cell of ~1% upon 40 h of AM1.5G exposure [16]. The GFP is known for being a photostable molecule [5,17] and thus, in both cases, resulting materials were found to be photostable.

4. Conclusions

Nature-based luminescent molecules present a great potential for applications in biotechnological and photovoltaic applications. To take advantage of their potential, it is necessary to overcome the drawbacks associated with their poor photochemical stability. A fundamental step to achieve this goal is their incorporation in solid materials, combining their outstanding photoluminescence features with a structure compatible with the processing in the solid state as thin films. We successfully incorporated two phycobiliproteins, R-PE and C-PC, and the xanthophyll FX into a poly(vinyl-alcohol) solid matrix. The emission spectra of the molecules in the visible range present the same profile in solution and after incorporation into the solid matrices. Moreover, in the case of FX, the incorporation into a solid matrix did not induce a significant change in the emission quantum yield (η) values, while in the case of both phycobiliproteins, the η values decrease when compared with the values measured for the proteins in aqueous solutions, which may be attributed to an aggregation mechanism occurring during the film's preparation. The matrices in solid state can be easily processed as thin films allowing the application of natural-based luminescent materials in a broader range of applications that require a chemically and optically stable material in solid state, such as downshifting layers and luminescent solar concentrators.

Supplementary Materials: The following are available online at https://www.mdpi.com/article/10.3390/app12125839/s1. Table S1. Absolute emission quantum yield (η) values of the as-prepared samples for the indicated excitation wavelengths (λ_{exc}, nm). Table S2. Absolute emission quantum yield (η) values of the samples after continuous exposition to AM1.5G radiation (t) for the indicated excitation wavelengths (λ_{exc}, nm). Figure S1. Calibration curves were used to the determination the concentration of each one of the extracts studied: (a) FX in ethanol, (b) R-PE in H_2O, and (c) C-PC in H_2O. Figure S2. Room-temperature (a) excitation and (b) emission spectra of R-PE in H_2O. Figure S3. Room-temperature (a) excitation and (b) emission spectra of R-PE/PVA sample. Figure S4. Room-temperature (a) excitation and (b) emission spectra of R-PE/alginate. Figure S5. Room-temperature (a) excitation and (b) emission spectra of C-PC in H_2O. Figure S6. Room-temperature (a) excitation and (b) emission spectra of C-PC/PVA. Figure S7. Room-temperature (a) excitation and (b) emission spectra of FX in ethanol. Figure S8. Room-temperature (a) excitation and (b) emission spectra of FX/PVA. Figure S9. Room-temperature emission decay curve of (a) R-PE in H_2O, (b) R-PE/PVA and (c) R-PE/alginate excited at 388 nm and monitored at 580 nm. The solid lines represent the data best fit ($R^2 > 0.99$), using a single-exponential function $I(t) = I_1 e^{-(t-t_0)/\tau_1}$ (t_0 = 13 ns, related to the excitation prompt). The respective residual plot is presented in (d). Figure S10. Room-temperature emission decay curve of (a) C-PC in H_2O and (b) C-PC/PVA excited at 388 nm and monitored at 670 nm. The solid lines represent the data best fit ($R^2 > 0.97$), using a single-exponential function $I(t) = I_1 e^{-(t-t_0)/\tau_1}$ (t_0 = 13 ns, related to the excitation prompt). The respective residual plots are presented in (c). Figure S11. Room-temperature emission decay curve of (a) FX in ethanol and (b) FX/PVA excited at 388 nm and monitored at 675 nm. The solid lines represent the data best fit ($R^2 > 0.99$), using a single-exponential function $I(t) = I_1 e^{-(t-t_0)/\tau_1}$ (t_0 = 20 ns, related to the excitation prompt). The respective residual plot is presented in (c).

Author Contributions: R.A.S.F. and S.P.M.V. conceived the idea of the experiment; experimental data were taken by S.F.H.C. and L.M.S.D.; the pigment's production was developed and optimized by I.P.E.M. and J.L.P.; the synthesis and processing were carried out by G.K., L.F., I.P.E.M., T.R.D., S.P.M.V., J.A.P.C., S.F.H.C., R.A.S.F. and S.P.M.V. co-wrote the paper with input from all authors. All authors have read and agreed to the published version of the manuscript.

Funding: This work was developed within the scope of the project CICECO-Aveiro Institute of Materials (UIDB/50011/2020, UIDP/50011/2020 & LA/P/0006/2020), Instituto de Telecomunicações (UID/EEA/50008/2021), CESAM (UIDP/50017/2020+UIDB/50017/2020+LA/P/0094/2020), SOLPOWINS—Solar-Powered Smart Windows for Sustainable Buildings (PTDC/CTM-REF/4304/2020), and REFINECYANO—Using biorefinery to value cyanobacteria pigments (PTDC/BTA-BTA/30914/2017), financed by national funds through the FCT/MEC and when appropriate co-financed by FEDER under the PT2020 Partnership through European Regional Development Fund (ERDF) in the frame of Operational Competitiveness and Internationalization Programme (POCI). I.P.E.M. and G.K. would like to thank Fundação para a Ciência e a Tecnologia for the doctoral grants SFRH/BD/123850/2016 and BD/REITORIA/9328/2020, respectively. S.F.H.C. would like to thank the European Space Agency (ESA STAR AO 2-1790/21/NL/GLC/ov). AMP Botas is acknowledged for preliminary optical measurements.

Institutional Review Board Statement: Not applicable.

Informed Consent Statement: Not applicable.

Conflicts of Interest: The authors declare no conflict of interest.

References

1. Ferreira, R.A.S.; Correia, S.F.H.; Monguzzi, A.; Liu, X.; Meinardi, F. Spectral converters for photovoltaics—What's ahead. *Mater. Today* **2020**, *33*, 105–121. [CrossRef]
2. McKenna, B.; Evans, R.C. Towards efficient spectral converters through materials design for luminescent solar devices. *Adv. Mater.* **2017**, *29*, 1606491. [CrossRef]
3. Jain, R.; Mathur, M.; Sikarwar, S.; Mittal, A. Removal of the hazardous dye rhodamine B through photocatalytic and adsorption treatments. *J. Environ. Manag.* **2007**, *85*, 956–964. [CrossRef] [PubMed]
4. Sadeghi, S.; Melikov, R.; Jalali, H.B.; Karatum, O.; Srivastava, S.B.; Conkar, D.; Firat-Karalar, E.N.; Nizamoglu, S. Ecofriendly and Efficient Luminescent Solar Concentrators Based on Fluorescent Proteins. *ACS Appl. Mater. Inter.* **2019**, *11*, 8710–8716. [CrossRef] [PubMed]

5. Correia, S.F.; Bastos, A.R.; Martins, M.; Macário, I.P.; Veloso, T.; Pereira, J.L.; Coutinho, J.A.; Ventura, S.P.; André, P.S.; Ferreira, R.A. Bio-based solar energy harvesting for onsite mobile optical temperature sensing in smart cities. *Adv. Sci.* **2022**, 2104801. [CrossRef]
6. Hernández-Rodríguez, M.A.; Correia, S.F.H.; Ferreira, R.A.S.; Carlos, L.D. A perspective on sustainable luminescent solar concentrators. *J. Appl. Phys.* **2022**, *131*, 140901. [CrossRef]
7. Weber, W.H.; Lambe, J. Luminescent greenhouse collector for solar radiation. *Appl. Opt.* **1976**, *15*, 2299–2300. [CrossRef]
8. Meinardi, F.; Bruni, F.; Brovelli, S. Luminescent solar concentrators for building-integrated photovoltaics. *Nat. Rev. Mater.* **2017**, *2*, 17072. [CrossRef]
9. Reisfeld, R.; Neuman, S. Planar solar-energy converter and concentrator based on uranyl-doped glass. *Nature* **1978**, *274*, 144–145. [CrossRef]
10. Yang, C.C.; Atwater, H.A.; Baldo, M.A.; Baran, D.; Barile, C.J.; Barr, M.C.; Bates, M.; Bawendi, M.G.; Bergren, M.R.; Borhan, B.; et al. Consensus statement: Standardized reporting of power-producing luminescent solar concentrator performance. *Joule* **2022**, *6*, 8–15. [CrossRef]
11. Debije, M.G.; Evans, R.C.; Griffini, G. Laboratory protocols for measuring and reporting the performance of luminescent solar concentrators. *Energ. Environ. Sci.* **2021**, *14*, 293–301. [CrossRef]
12. Debije, M.G.; Rajkumar, V.A. Direct versus indirect illumination of a prototype luminescent solar concentrator. *Sol. Energy* **2015**, *122*, 334–340. [CrossRef]
13. Mulder, C.L.; Theogarajan, L.; Currie, M.; Mapel, J.K.; Baldo, M.A.; Vaughn, M.; Willard, P.; Bruce, B.D.; Moss, M.W.; McLain, C.E.; et al. Luminescent Solar Concentrators Employing Phycobilisomes. *Adv. Mater.* **2009**, *21*, 3181–3185. [CrossRef]
14. Bose, R.; Gonzalez, M.; Jenkins, P.; Walters, R.; Morseman, J.; Moss, M.; McLain, C.; Linsert, P.; Buchtemann, A.; Chatten, A.J.; et al. Resonance Energy Transfer in Luminescent Solar Concentrators. In Proceedings of the 35th IEEE Photovoltaic Specialists Conference, Honolulu, HI, USA, 20–25 June 2010.
15. Frias, A.R.; Correia, S.F.H.; Martins, M.; Ventura, S.P.M.; Pecoraro, E.; Ribeiro, S.L.; Andre, P.S.; Ferreira, R.A.S.; Coutinho, J.A.P.; Carlos, L.D. Sustainable liquid luminescent solar concentrators. *Adv. Sustain. Syst.* **2019**, *3*, 1800134. [CrossRef]
16. Frias, A.R.; Pecoraro, E.; Correia, S.F.H.; Minas, L.M.G.; Bastos, A.R.; Garcia-Revilla, S.; Balda, R.; Ribeiro, S.J.L.; Andre, P.S.; Carlos, L.D.; et al. Sustainable luminescent solar concentrators based on organic-inorganic hybrids modified with chlorophyll. *J. Mater. Chem. A* **2018**, *6*, 8712–8723. [CrossRef]
17. Carlos, C.P.A.; Correia, S.F.H.; Martins, M.; Savchuk, O.A.; Coutinho, J.A.P.; André, P.S.; Nieder, J.B.; Ventura, S.P.M.; Ferreira, R.A.S. Environmentally friendly luminescent solar concentrators based on optically efficient and stable green fluorescent protein. *Green. Chem.* **2020**, *22*, 4943–4951. [CrossRef]
18. Bharmoria, P.; Correia, S.F.H.; Martins, M.; Hernández-Rodríguez, M.A.; Ventura, S.P.M.; Ferreira, R.A.S.; Carlos, L.D.; Coutinho, J.A.P. Protein Co-habitation: Improving the Photo-Chemical Stability of R-Phycoerythrin in Solid State. *J. Phys. Chem. Lett.* **2020**, *11*, 6249–6255. [CrossRef]
19. Keeling-Tucker, T.; Brennan, J.D. Fluorescent probes as reporters on the local structure and dynamics in sol-gel-derived nanocomposite materials. *Chem. Mater.* **2001**, *13*, 3331–3350. [CrossRef]
20. Chen, Z.P.; Samuelson, L.A.; Akkara, J.; Kaplan, D.L.; Gao, H.; Kumar, J.; Marx, K.A.; Tripathy, S.K. Sol-Gel Encapsulated Light-Transducing Protein Phycoerythrin—A New Biomaterial. *Chem. Mater.* **1995**, *7*, 1779–1783. [CrossRef]
21. Keeling-Tucker, T.; Rakic, M.; Spong, C.; Brennan, J.D. Controlling the material properties and biological activity of lipase within sol-gel derived bioglasses via organosilane and polymer doping. *Chem. Mater.* **2000**, *12*, 3695–3704. [CrossRef]
22. Chen, Z.P.; Kaplan, D.L.; Yang, K.; Kumar, J.; Marx, K.A.; Tripathy, S.K. Phycobiliproteins encapsulated in sol-gel glass. *J. Sol-Gel Sci. Technol.* **1996**, *7*, 99–108. [CrossRef]
23. Pradeep, H.N.; Nayak, C.A. Enhanced stability of C-phycocyanin colorant by extrusion encapsulation. *J. Food Sci. Techol.* **2019**, *56*, 4526–4534. [CrossRef]
24. Wang, X.B.; Li, Z.Y.; Ying, W.; Chen, D.K.; Li, P.P.; Deng, Z.; Peng, X.S. Blue metal-organic framework encapsulated denatured R-phycoerythrin proteins for a white-light-emitting thin film. *J. Mater. Chem. C* **2020**, *8*, 240–246. [CrossRef]
25. Sui, Y.; Gu, Y.; Lu, Y.J.; Yu, C.X.; Zheng, J.; Qi, H. Fucoxanthin@Polyvinylpyrrolidone Nanoparticles Promoted Oxidative Stress-Induced Cell Death in Caco-2 Human Colon Cancer Cells. *Mar. Drugs* **2021**, *19*, 92. [CrossRef]
26. Jaswir, I.; Noviendri, D.; Taher, M.; Mohamed, F.; Octavianti, F.; Lestari, W.; Mukti, A.G.; Nirwandar, S.; Almansori, B.B.H. Optimization and Formulation of Fucoxanthin-Loaded Microsphere (F-LM) Using Response Surface Methodology (RSM) and Analysis of Its Fucoxanthin Release Profile. *Molecules* **2019**, *24*, 947. [CrossRef]
27. Nichols, H.W. Growth media—Freshwater. In *Handbook of Phycological Methods: Culture Methods and Growth Measurements*; Stein, J.R., Ed.; Cambridge University Press: Cambridge, UK, 1973; pp. 7–24.
28. Vaz, B.M.C.; Martins, M.; Mesquita, L.M.D.; Neves, M.C.; Fernandes, A.P.M.; Pinto, D.C.G.A.; Neves, M.G.P.M.S.; Coutinho, J.A.P.; Ventura, S.P.M. Using aqueous solutions of ionic liquids as chlorophyll eluents in solid-phase extraction processes. *Chem. Eng. J.* **2022**, *428*, 131073. [CrossRef]
29. Bai, X.; Caputo, G.; Hao, Z.; Freitas, V.T.; Zhang, J.; Longo, R.L.; Malta, O.L.; Ferreira, R.A.S.; Pinna, N. Efficient and tuneable photoluminescent boehmite hybrid nanoplates lacking metal activator centres for single-phase white LEDs. *Nat. Commun.* **2014**, *5*, 5702. [CrossRef]

30. Martins, M.; Vieira, F.A.; Correia, I.; Ferreira, R.A.S.; Abreu, H.; Coutinho, J.A.P.; Ventura, S.P.M. Recovery of phycobiliproteins from the red macroalga Gracilaria sp using ionic liquid aqueous solutions. *Green. Chem.* **2016**, *18*, 4287–4296. [CrossRef]
31. Rowan, K.S. *Photosynthetic Pigments of Algae*, 1st ed.; Cambridge University Press Archive: Cambridge, UK, 1989.
32. Egorov, V.V. Theory of the J-band: From the Frenkel exciton to charge transfer. *Phys. Procedia* **2009**, *2*, 223–326. [CrossRef]
33. Stryjewski, W.; Barkley, M.D. Solid-State Fluorescence Lifetime Measurements. *Time-Resolv. Laser Spectrosc. Biochem. II* **1990**, *1204*, 244–246. [CrossRef]
34. Glazer, A.N. Light Harvesting by Phycobilisomes. *Annu. Rev. Biophys. Biol.* **1985**, *14*, 47–77. [CrossRef] [PubMed]